Synthesis and Alignment of Silver Nanorods and Nanowires and the Formation of Pt, Pd, and Core/Shell Structures by Galvanic Exchange Directly on Surfaces

Grzegorz W. Sławiński and Francis P. Zamborini*

Department of Chemistry, University of Louisville, Louisville, Kentucky 40292

Received May 31, 2007. In Final Form: July 16, 2007

Here we describe the synthesis of Ag nanorods (NRs) (aspect ratio <20) and nanowires (NWs) (aspect ratio ≥20) directly on surfaces by seed-mediated growth. The procedure involves attaching gold seed nanoparticles (Au NPs) to 3-mercaptopropyltrimethoxysilane (MPTMS)-functionalized silicon or glass surfaces and growing them into NRs/NWs by placing the substrates into a solution containing cetyltrimethylammonium bromide (CTAB), silver nitrate, and ascorbic acid with the pH ranging from 7 to 12. Under our conditions, Ag NRs/NWs grow optimally at pH 10.6 with a 3% yield, where spherical, triangular, and hexagonal nanostructures represent the other byproducts. The length of Ag NRs/NWs ranges from 50 nm to more than 10 μm, the aspect ratio (AR) ranges from 1.4 to >300, and the average diameter is approximately 35 nm. Approximately 40% of the 1D structures are NRs, and 60% are NWs as defined by their ARs. We also report the alignment of Ag NRs/NWs directly on surfaces by growing the structures on amine-functionalized Si(100) surfaces after an amidation reaction with acetic acid and a method to improve the percentage of Ag NRs/NWs on the surface by removing structures of other shapes with adhesive tape. Surface-grown Ag NRs/NWs also react with salts of palladium, platinum, and gold via galvanic exchange reactions to form high-surface-area 1D structures of the corresponding metal. The combination of the seed-mediated growth of Ag on Au NRs followed by the galvanic exchange of Ag with Pd leads to interesting core/shell NRs grown directly on surfaces. We used scanning electron microscopy, UV−vis spectroscopy, and X-ray photoelectron spectroscopy to characterize the surface-grown nanostructures.

Introduction

One-dimensional (1D) nanostructures[1] have recently gained a tremendous amount of attention because of their fascinating chemistry, properties, and potential use in a wide range of electronic,[2] analytical,[3−5] and biomedical[6] applications. Single- or multicomponent nanoscale materials composed of semiconductors, carbon, polymers, and metals show unique electronic, optical, and magnetic properties that vary with the composition, size, and shape of the nanostructure. Our research focuses on the synthesis of 1D metal nanostructures and the development of simple chemical methods for assembling,[7] patterning,[8] and aligning the structures,[9] creating nanoscale 1D heterojunctions between different materials[10,11] and forming electrical contacts with the nanostructures. Advances in these areas will lead to a better fundamental understanding of structure−function relationships within 1D materials and their use in electronics, sensing, catalysis, and electrochemical applications.

There are generally three methods for assembling 1D nanostructures on surfaces: lithography, synthesis of 1D structures followed by assembly on surfaces from a solution, and synthesis of 1D structures directly on surfaces from a surface-bound catalyst. The third approach has been commonly used to synthesize semiconductor nanowires (NWs) and carbon nanotubes directly on surfaces by the well-known vapor−liquid−solid (VLS) growth mechanism;[12−15] however, these methods do not work for metal structures. Murphy and co-workers recently developed a solution method for synthesizing 1D metal nanorods (NRs) and NWs from presynthesized metal nanoparticle "seeds", which act as a catalyst in this process known as seed-mediated growth.[16] Because the synthesis occurs by preferential metal reduction on a catalyst particle, the procedure is ideal for synthesizing metal 1D structures directly on surfaces from surface-attached seeds. Taub et al. first described the synthesis of Au nanorods (NRs) directly on surfaces from surface-bound Au nanoparticle seeds,[17] followed by our group[7−10,18] and others.[19,20] We synthesized,[7] patterned,[8] and aligned[9] Au NRs directly on surfaces with control over the average length and AR and also demonstrated the formation of heterojunctions with Au NRs and CNT or GaAs by combining seed-mediated growth with vapor-phase synthesis and chemical

* Author to whom correspondence should be addressed. Fax: 502-852-8149. E-mail: f.zamborini@louisville.edu.

(1) Xia, Y.; Yang, P.; Sun, Y.; Wu, Y.; Mayers, B.; Gates, B.; Yin, Y.; Kim, F.; Yan, H. *Adv. Mater.* **2003**, *15*, 353−389.
(2) Zheng, G.; Lu, W.; Jin, S.; Lieber, C. M. *Adv. Mater.* **2004**, *16*, 1890−1893.
(3) Cui, Y.; Wei, Q.; Park, H.-Y.; Lieber, C. M. *Science* **2001**, *293*, 1289−1292.
(4) Hahm, J.-i.; Lieber, C. M. *Nano Lett.* **2004**, *4*, 51−54.
(5) Favier, F.; Walter, E. C.; Zach, M. P.; Benter, T.; Penner, R. M. *Science* **2001**, *293*, 2227.
(6) Huang, X.; El-Sayed, I. H.; Qian, W.; El-Sayed, M. A. *J. Am. Chem. Soc.* **2006**, *128*, 2115−2120.
(7) Wei, Z.; Mieszawska, A. J.; Zamborini, F. P. *Langmuir* **2004**, *20*, 4322−4326.
(8) Mieszawska, A. J.; Zamborini, F. P. *Chem. Mater.* **2005**, *17*, 3415−3420.
(9) Mieszawska, A. J.; Slawinski, G. W.; Zamborini, F. P. *J. Am. Chem. Soc.* **2006**, *128*, 5622−5623.
(10) Mieszawska, A. J.; Jalilian, R.; Sumanasekera, G. U.; Zamborini, F. P. *J. Am. Chem. Soc.* **2005**, *127*, 10822−10823.
(11) Mieszawska, A. J.; Jalilian, R.; Sumanasekera, G. U.; Zamborini, F. P. *Small* **2007**, *3*, 722−756.
(12) Lauhon, L. J.; Gudiksen, M. S.; Lieber, C. M. *Philos. Trans. R. Soc. London, Ser. A* **2004**, *362*, 1247−1260.
(13) Law, M.; Goldberger, J.; Yang, P. *Annu. Rev. Mater. Res.* **2004**, *34*, 83−122.
(14) Rao, C. N. R.; Deepak, F. L.; Gundiah, G.; Govindaraj, A. *Prog. Solid State Chem.* **2003**, *31*, 5−147.
(15) Samuelson, L. *Mater. Today* **2003**, *6*, 22−31.
(16) Jana, N. R.; Gearheart, L.; Murphy, C. J. *J. Phys. Chem. B* **2001**, *105*, 4065−4067.
(17) Taub, N.; Krichevski, O.; Markovich, G. *J. Phys. Chem. B* **2003**, *107*, 11579−11582.
(18) Wei, Z.; Zamborini, F. P. *Langmuir* **2004**, *20*, 11301−11304.
(19) Liao, H.; Hafner, J. H. *J. Phys. Chem. B* **2004**, *108*, 19276−19280.
(20) Shopova, S. I.; Blackledge, C. W.; Rosenberger, A. T.; Materer, N. F. *Appl. Phys. Lett.* **2006**, *89*, 023120-1−023120-3.

10.1021/la701606p CCC: $37.00 © 2007 American Chemical Society
Published on Web 08/31/2007

assembly.[10,11] The general procedure involves attaching presynthesized 3−5-nm-diameter Au seed nanoparticles to a desired substrate and then growing the seeds into larger structures by reducing $AuCl_4^-$ preferentially on the Au seeds with ascorbic acid in the presence of cetyltrimethylammonium bromide (CTAB), which is the same method as that described by Murphy and co-workers for seed-mediated growth in solution[16] except that the seed particles are surface-bound instead of in solution.

The goal of this work was to extend our procedure for synthesizing Au NRs directly on surfaces to other metals in order to broaden the potential applications for these structures in catalysis and sensing. Here we describe the synthesis of Ag NRs and NWs directly on surfaces using a similar approach to that used for Au. There are several reported approaches to the synthesis of Ag into 1D nanostructures, including UV irradiation,[21,22] a surfactant method,[23−26] microwave heating,[27−29] the polyol process,[29−33] and seedless and surfactantless chemical synthesis[34] or by using DNA molecules, carbon nanotubes, silica gel, membranes, or mesoporous materials as templates.[35−40] Most of these procedures lead to a suspension of nanostructures requiring postsynthesis assembly for application. Postsynthesis assembly is often challenging because of aggregation, uncontrolled placement on surfaces, and the need to remove impurities or side products. Our approach is a simple benchtop chemical method that allows for easy assembly of isolated 1D Ag nanostructures. The direct growth on surfaces is also amenable to patterning,[8] alignment,[9] the formation of heterojunctions,[10,11] and for following the growth process by surface microscopy.[18,19]

There are a few other examples of Ag NRs or NWs grown directly on surfaces by seed-mediated growth. For example, Aslan et al. recently attached Ag seed particles to amine-coated substrates and studied the metal-enhanced fluorescence of the surface-grown Ag NRs.[41] Lee et al. grew Ag NRs from Ag seeds attached to thiol-coated surfaces, focusing on the effect of Ag seed coverage and reaction time, and they imaged the structures by dark-field microscopy.[42] In this report, we study the effect of pH by growing the structures in buffered solutions, growing aligned Ag NRs/NWs on surfaces, and utilize Ag NRs/NWs as templates for forming other metal structures with desirable catalytic and sensing properties. Other related approaches for Ag NW synthesis directly on surfaces in the literature include the electroless deposition of Ag on a surface-bound DNA network[35] or a DNA template assembled across an electrode gap[36] and the synthesis of Ag NWs in a thin surfactant solution film.[43]

The ability to grow Ag 1D nanostructures is important because Ag has higher conductivity, high reflectivity, and is cheaper than Au, which may be important for certain applications. It has also been found to be useful for ammonium sensing[44,45] and biosensing[46−48] and is easier to oxidize, giving it semiconducting properties that may prove to be more useful in chemical sensing and nanoelectronics applications. Like Au, Ag is useful in plasmonics applications[49] and surface-enhanced Raman spectroscopy,[50] but it is also important in catalysis[51] and as potential electrical contacts in nanoscale devices.[52] An extra benefit is that, unlike Au, Ag can undergo galvanic exchange reactions with Pd or Pt salts to form pure Pd, Pt, PdAg, or PtAg alloy 1D nanostructures,[53−59] extending the different types of metal further and opening up the possibility of studying catalysis[60−62] and other sensing applications (such as H_2 sensing).[5,63−65]

Experimental Section

Chemicals and Materials. Silver nitrate ($AgNO_3$, 99+%), sodium borohydride ($NaBH_4$, 98%), potassium tetrachloropalladate(II) (K_2PdCl_4, 98%), 4-(dimethylamino)pyridine (99%) (DMAP), and L-ascorbic acid (99.9%) were purchased from Sigma-Aldrich. Hydrogen tetrachloroaureate trihydrate ($HAuCl_4 \cdot 3H_2O$) was synthesized according to a literature procedure.[66] Citric acid, trisodium salt was purchased from Bio-Rad Laboratories. Sodium phosphate dibasic and sodium phosphate tribasic were purchased from Fisher Scientific Company. Platinum potassium chloride (K_2PtCl_4, 99.9%) was purchased from ROC/RIC (Research Organic/Inorganic Chemical Co). *N*,*N*′-Dicyclohexylcarbodiimide (DCC) (99%) was purchased from Fluka. Methylene chloride (99.5%), hydrogen peroxide (H_2O_2

(21) Jiang, X.; Xie, Y.; Lu, J.; Zhu, L.; He, W.; Qian, Y. *J. Mater. Chem.* **2001**, *11*, 1775−1777.
(22) Zhou, Y.; Yu, S. H.; Wang, C. Y.; Li, X. G.; Zhu, Y. R.; Chen, Z. Y. *Adv. Mater.* **1999**, *11*, 850−852.
(23) Murphy, C. J.; Sau, T. K.; Gole, A. M.; Orendoff, C. J.; Gao, J.; Gou, L.; Hunyadi, S. E.; Li, T. *J. Phys. Chem. B* **2005**, *109*, 13857−13870.
(24) Jana, N. R.; Gearheart, L.; Murphy, C. J. *Chem. Commun.* **2001**, 617−618.
(25) Ni, C.; Hassan, P. A.; Kaler, E. W. *Langmuir* **2005**, *21*, 3334−3337.
(26) Graff, A.; Wagner, D.; Ditlbacher, H.; Kreibig, U. *Eur. Phys. J. D* **2005**, *34*, 263−269.
(27) Liu, F.-K.; Huang, P.-W.; Chang, Y.-C.; Ko, C.-J.; Ko, F.-H.; Chu, T.-C. *J. Cryst. Growth* **2005**, *273*, 439−445.
(28) Gou, L.; Chipara, M.; Zaleski, J. M. *Chem. Mater.* **2007**, *19*, 1755−1760.
(29) Tsuji, M.; Matsumoto, K.; Miyamae, N.; Tsuji, T.; Zhang, X. *Cryst. Growth Des.* **2007**, *7*, 311−320.
(30) Wiley, B.; Sun, Y.; Mayers, B.; Xia, Y. *Chem.*−*Eur. J.* **2005**, *11*, 454−463.
(31) Sun, Y.; Gates, B.; Mayers, B.; Xia, Y. *Nano Lett.* **2002**, *2*, 165−168.
(32) Sun, Y.; Xia, Y. *Science* **2002**, *298*, 2176−2179.
(33) Sun, Y.; Mayers, B.; Herricks, T.; Xia, Y. *Nano Lett.* **2003**, *3*, 955−960.
(34) Caswell, K. K.; Bender, C. M.; Murphy, C. J. *Nano Lett.* **2003**, *3*, 667−669.
(35) Wei, G.; Zhou, H.; Liu, Z.; Song, Y.; Wang, L.; Sun, L.; Li, Z. *J. Phys. Chem. B* **2005**, *109*, 8738−8743.
(36) Braun, E.; Eichen, Y.; Sivan, U.; Ben-Yoseph, G. *Nature* **1998**, *391*, 775−778.
(37) Ugarte, D.; Chatelain, A.; deHeer, W. A. *Science* **1996**, *274*, 1897−1899.
(38) Bhattacharyya, S.; Saha, S. K.; Chakravorty, D. *Appl. Phys. Lett.* **2000**, *77*, 3770−3772.
(39) Han, Y.-J.; Kim, J. M.; Stucky, G. D. *Chem. Mater.* **2000**, *12*, 2068−2069.
(40) Huang, M. H.; Choudrey, A.; Yang, P. *Chem. Commun.* **2000**, 1063−1064.
(41) Aslan, K.; Leonenko, Z.; Lakowicz, J. R.; Geddes, C. D. *J. Phys. Chem. B* **2005**, *109*, 3157−3162.
(42) Lee, K.-H.; Huang, K.-M.; Tseng, W.-L.; Chiu, T.-C.; Lin, Y.-W.; Chang, H.-T. *Langmuir* **2007**, *23*, 1435−1442.
(43) Krichevski, O.; Tirosh, E.; Markovich, G. *Langmuir* **2006**, *22*, 867−870.
(44) Murray, B. J.; Li, Q.; Newberg, J. T.; Hemminger, J. C.; Penner, R. M. *Chem. Mater.* **2005**, *17*, 6611−6618.
(45) Murray, B. J.; Newberg, J. T.; Walter, E. C.; Li, Q.; Hemminger, J. C.; Penner, R. M. *Anal. Chem.* **2005**, *77*, 5205−5214.
(46) Keating, C. D.; Natan, M. J. *Adv. Mater.* **2003**, *15*, 451−454.
(47) Nicewarner-Pena, S. R.; Freeman, G. R.; Reiss, B. D.; He, L.; Pena, D. J.; Walton, I. D.; Cromer, R.; Keating, C. D.; Natan, M. J. *Science* **2001**, *294*, 137−141.
(48) Penn, S. G.; He, L.; Natan, M. J. *Curr. Opin. Chem. Biol.* **2003**, *7*, 609−615.
(49) Maier, S. A.; Kik, P. G.; Atwater, H. A.; Meltzer, S.; Harel, E.; Koel, B. E.; Requicha, A. A. G. *Nat. Mater.* **2003**, *2*, 229−232.
(50) Tao, A.; Kim, F.; Hess, C.; Goldberger, J.; He, R.; Sun, Y.; Xia, Y.; Yang, P. *Nano Lett.* **2003**, *3*, 1229−1233.
(51) Chen, Z.; Gao, Q.; Gao, D.; Wei, Q.; Ruan, M. *Mater. Lett.* **2005**, *60*, 1816−1822.
(52) Prokes, S. M.; Wang, K. L. *MRS Bull.* **1999**, *24*, 13−14.
(53) Sun, Y.; Mayers, B. T.; Xia, Y. *Nano Lett.* **2002**, *2*, 481−485.
(54) Sun, Y.; Mayers, B.; Xia, Y. *Adv. Mater.* **2003**, *15*, 641−646.
(55) Sun, Y.; Xia, Y. *J. Am. Chem. Soc.* **2004**, *126*, 3892−3901.
(56) Sun, Y.; Tao, Z.; Chen, J.; Herricks, T.; Xia, Y. *J. Am. Chem. Soc.* **2004**, *126*, 5940−5941.
(57) Chen, J.; Willey, B.; McLellan, J.; Xiong, Y.; Li, Z.-Y.; Xia, Y. *Nano Lett.* **2005**, *5*, 2058−2062.
(58) Sun, Y.; Xia, Y. *Adv. Mater.* **2004**, *16*, 264−268.
(59) Sun, Y.; Willey, B.; Li, Z.-Y.; Xia, Y. *J. Am. Chem. Soc.* **2004**, *126*, 9399−9406.
(60) Liu, F.; Lee, J. Y.; Zhou, W. *J. Phys. Chem. B* **2004**, *108*, 17959−17963.
(61) Liu, F.; Lee, J. Y.; Zhou, W. *Adv. Funct. Mater.* **2005**, *15*, 1459−1464.
(62) Liu, F.; Lee, J. Y.; Zhou, W. J. *Small* **2006**, *2*, 121−128.
(63) Ibañez, F. J.; Zamborini, F. P. *Langmuir* **2006**, *22*, 9789−9796.
(64) Walter, E. C.; Favier, F.; Penner, R. M. *Anal. Chem.* **2002**, *74*, 1546−1553.
(65) Sun, Y.; Tao, Z.; Chen, J.; Herricks, T.; Xia, Y. *J. Am. Chem. Soc.* **2004**, *126*, 5940−5941.
(66) Block, B. P. *Inorg. Synth.* **1953**, *4*, 14−17.

30% solution), and 2-propanol (HPLC grade, 99.99%) were purchased from EMD. Cetyltrimethylammonium bromide (CTAB) was purchased both from Sigma-Aldrich (~97%) and Fluka (99%). Note that the source of CTAB is important in obtaining 1D nanostructures. Using CTAB purchased from Sigma-Aldrich at the beginning of this project and Fluka resulted in the reproducible synthesis of Ag NRs and NWs. Sigma-Aldrich recently altered their production method for CTAB, and now the use of their product does not produce Ag NRs/NWs. We are currently exploring the reason for this because it may lead to a better understanding of the NR/NW growth mechanism and improvements in yields and dispersity. NANOpure ultrapure water (resistivity of 18 MΩ cm) was used for all aqueous solutions.

Preparation of Gold Seed Solution. We used the procedure of Murphy and co-workers to prepare a solution of 3−5-nm-diameter Au nanoparticle (NP) seeds.[16,67] A 20 mL aqueous solution containing 2.5×10^{-4} M $HAuCl_4$ and 2.5×10^{-4} M trisodium citrate was prepared in a scintillation vial. Ice-cold 0.1 M $NaBH_4$ solution (0.6 mL) was injected at once into the solution, and it was stirred vigorously for 2 h. The solution changed color from yellow to red immediately after adding $NaBH_4$. The particles in this solution were used as the seed solution in the following section within 2−5 h after preparation. The average particle size was 3−5 nm according to the literature and our previous work.[7,16,18,67]

Preparation of Silver Growth Solution. CTAB (0.29 g, 8×10^{-4} mol) was dissolved by sonication in 10 mL of a 0.2 M ionic strength phosphate buffer with pH ranging from 7 to 12,[68] leading to an ~0.08 M CTAB solution after adding 0.25 mL of 0.01 M $AgNO_3$ and 0.50 mL of freshly prepared 0.1 M ascorbic acid solutions sequentially. The solution pH values reported in the article are those measured before adding silver nitrate and ascorbic acid. The actual values are slightly lower because of the addition of ascorbic acid. The growth solution remained colorless or a very slight yellow color throughout the whole process of the growth procedure, indicating that the reduction of Ag^+ to metallic Ag^0 did not occur in solution to a significant extent.

Preparation of Glass and Silicon Surfaces for the Growth Procedure. A glass or Si/SiO_x substrate was cleaned in 3:1 H_2SO_4/30% H_2O_2 ***(Caution! This solution, known as piranha, reacts violently with organic compounds.)***, rinsed thoroughly with nanopure water and 2-propanol, and dried under N_2. The glass or Si/SiO_x was then functionalized by heating for 30 min in a solution containing 10 mL of 2-propanol, 100 μL of mercaptopropyltrimethoxysilane (MPTMS), and 4 to 5 drops of nanopure water. After thoroughly rinsing with 2-propanol and drying under N_2, the [glass or Si/SiO_x]/MPTMS substrate was placed directly in an aqueous solution of Au NP seed for 20 min. The functionalized [glass or Si/SiO_x]/MPTMS/Au NP slide was removed, rinsed with water, dried with N_2, and placed in the Ag growth solution immediately after ascorbic acid was added (see previous section) at 28 °C for 30 min. It was removed, rinsed with water, and dried under N_2 before analysis.

Alignment of AgNRs on the Surface. Aligned Ag NRs/NWs were synthesized directly on Si(100) substrates as described previously.[9] The procedure for preparing samples for aligned Ag NRs followed the preparation of the glass or Si/SiO_x surface as described earlier, except that aminopropyltriethoxysilane (APTES) was used instead of MPTMS. The substrate was then placed for 4 h into a 10 mL methylene chloride solution containing 10 mM acetic acid, 20 mM dicyclohexylcarbodiimide (DCC), and 20 mM dimethylamino pyridine (DMAP). After the substrate was removed, rinsed with methylene chloride and 2-propanol, and dried under N_2, it was placed into Au NP seed solution for 20 min, rinsed with water, dried under N_2, and placed into Ag growth solution for 30 min at 28 °C.

Galvanic Exchange between Ag and Pt, Pd, and Au Salts. Ag NRs/NWs were prepared as described previously and placed into aqueous solutions of 0.005 M K_2PtCl_4, K_2PdCl_4, or $HAuCl_4$ for the exchange of Pt, Pd, and Au, respectively. The samples were monitored by UV−vis spectroscopy with time for 30 min. After the sample was removed at a given time, it was rinsed with nanopure H_2O, dried under N_2, and characterized by UV−vis spectroscopy and scanning electron microscopy (SEM). Au/Pd core/shell NRs were prepared by first synthesizing Au NRs directly on glass or Si/SiO_x surfaces according to our previously described procedure.[7,8,18] After the surfaces were rinsed with water, Ag was deposited as a shell on the Au NRs by placing the samples into an Ag growth solution at pH 10.6 for 30 min. This step was repeated up to nine times to produce controlled amounts of Ag in the shell as indicated later in the text. Next, the samples were thoroughly rinsed with water and placed into an aqueous solution of 0.005 M K_2PdCl_4 for 5 min in order to exchange the Ag shell with Pd, leading to Au/Pd core/shell structures directly on the surface. The samples were removed, rinsed with water, and dried under N_2 before analysis.

Scheme 1. Procedure for Growing Surface-Attached Ag Nanostructures

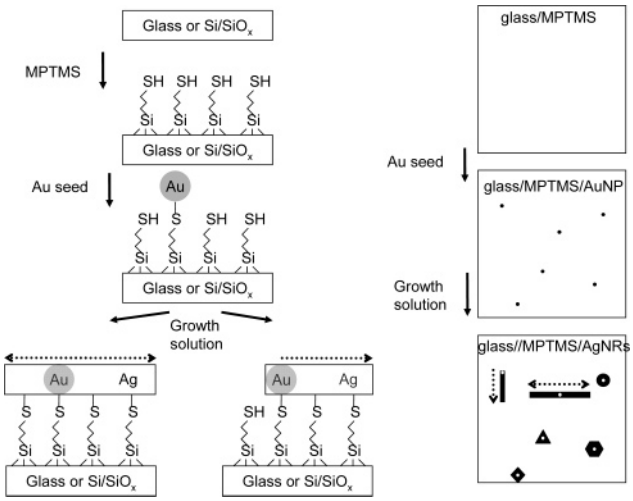

Instrumentation. Electron microscopy images were obtained at different magnifications using a Carl Zeiss SMT AG Supra 35VP field-emission scanning electron microscope (FESEM) operating at an accelerating voltage of 20.00 kV and using an in-lens ion annular secondary electron detector. Atomic force microscopy (AFM) images were obtained with a Veeco Metrology Multimode Nanoscope IIIA operating in tapping mode. UV−vis spectra were obtained using a Varian Cary 50 Bio UV−visible spectrophotometer. X-ray photoelectron spectroscopy (XPS) data were obtained using a VG Surface Analysis System from Thermo Fisher Scientific. Surface compositional analysis of the samples was performed using Mg Kα X-rays (1253.6 eV) and a spectrometer pass energy of 50 meV.

Results and Discussion

Effect of pH on the Growth of Ag NRs/NWs. We grew Ag NRs/NWs directly on surfaces using our previously described procedure for Au with a few slight variations.[7] The procedure is illustrated in Scheme 1. First, the glass or Si/SiO_x was functionalized with 3-MPTMS and Au seed particles as shown in steps 1 and 2, respectively. These two steps are identical to the procedure for growing Au NRs on surfaces. The substrate was then placed into an Ag growth solution for 30 min, which consists of 10 mL of 0.08 M cetyltrimethylammonium bromide (CTAB) dissolved in 0.2 M ionic strength (pH 7−12) phosphate buffer, 0.25 mL of 0.1 M $AgNO_3$, and 0.5 mL of 0.1 M ascorbic acid. This is similar to the Au NR growth solution except that the CTAB concentration is slightly lower than 0.1 M for Au, the Ag^+ concentration is slightly lower than the $AuCl_4^-$ concentration (0.45 mL of 0.1 M for Au), the ascorbic acid is 10-fold higher (0.05 mL of 0.1 M ascorbic acid for Au), and the time in the growth solution is 30 min for Ag as opposed to 60 min for Au. The other major difference is that we buffered the growth solution

(67) Gole, A.; Murphy, C. J. *Chem. Mater.* **2004**, *16*, 3633−3640.
(68) Christian, G. D.; Purdy, W. C. *J. Electroanal. Chem.* **1962**, *3*, 363−367.

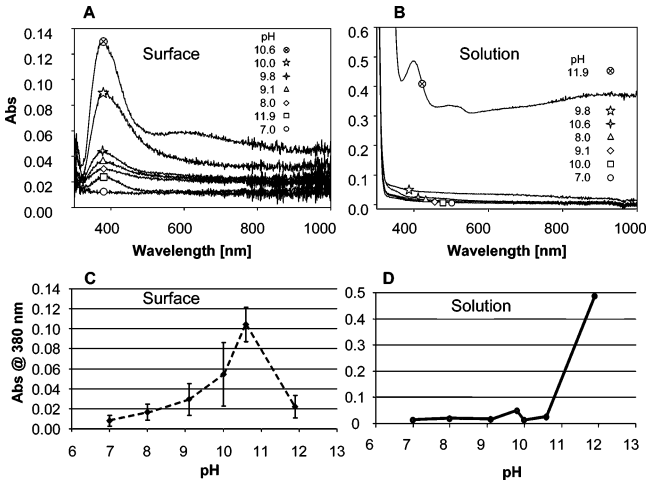

Figure 1. UV−vis spectra of (A) glass slides coated with Au seed particles that were placed in Ag growth solutions at the indicated pH for 30 min and (B) the corresponding Ag growth solutions. Plots of the absorbance at 380 nm of (C) the glass slides and (D) the growth solutions as a function of pH.

to a pH between 7 and 12 whereas the Au growth solution is not buffered and is generally slightly acidic (pH <7). Because the standard reduction potential for Ag^+ is more negative than that for $AuCl_4^-$, it requires a larger reducing strength to reduce it to the metallic Ag^0 form. The reducing strength of ascorbic acid increases as the pH increases and a larger amount of ascorbate is present in solution. Murphy and co-workers previously added small amounts of NaOH to the growth solution,[69] and Lee and co-workers[70] used buffers to increase the pH to a regime where the seed-mediated growth of Ag was possible in solution-phase growth methods. Previous examples of Ag NRs grown directly on surfaces used solutions with NaOH added.[41,42] We had trouble with reproducibly synthesizing Ag NRs/NWs by adding NaOH to solutions, which we believe was due to the uncertainty in the NaOH concentration. We therefore decided to use buffered solutions to gain better control over the pH and determine the optimal conditions for the seed-mediated growth of Ag 1D structures directly on surfaces with high reproducibility.

Figure 1 shows the UV−vis spectra of glass/MPTMS/Au NP seed samples (frame A) and the corresponding growth solutions (frame B) after the samples were placed in growth solutions of different pH for 30 min. In Figure 1A, the peak at 380 nm represents the transverse plasmon band for Ag 1D structures and particles. The absorbance of this peak increases as the pH increases from 7.0 to 10.6 but then decreases again at pH 11.9. The increase from pH 7.0 to 10.6 is due to the increase in the reducing strength of ascorbic acid, which causes more growth to occur on the substrate during the 30 min experiment. The absorbance on the glass slide decreases at pH 11.9 because the reducing strength is large enough to cause the nucleation and growth of Ag structures by the reduction of Ag^+ throughout the entire growth solution. This reduces the bulk solution Ag^+ concentration and hence the flux of Ag^+ at the surface, which reduces the amount of Ag growth occurring on the glass slide. Overall, these data show that growth does not occur appreciably below pH 8.0, from pH 8.0 to 10.6 growth occurs mainly by seed-mediated growth on the surface-attached Au NP seeds, and above pH 11.0 the nucleation and growth of Ag nanostructures occurs throughout the entire solution and not only by seed-mediated growth on the surface.

The UV−vis spectra of the growth solutions shown in Figure 1B confirm the behavior just described. In this case, the absorbance of the growth solution is extremely low for solutions of pH 10.6 and lower. (See Figure S1 in Supporting Information for an expanded view of these spectra.) The spectra are mostly featureless as expected for a seed-mediated growth process where the deposition of Ag occurs only at the seed particles, which are attached to the substrate. However, the spectrum for the growth solution at pH 11.9 shows a large absorbance at 380 nm, confirming the reduction of Ag^+ to Ag^0 nanostructures throughout the bulk solution, consistent with minimal growth on the surface in Figure 1A (□). Frames C and D of Figure 1 show plots of the absorbance at 380 nm as a function of pH for the glass substrates and corresponding growth solutions, respectively. Part C of Figure 1 shows the maximum growth on the glass substrate at pH 10.6, and part D of Figure 1 shows that above pH 10.6 there is a significant amount of nucleation and growth of Ag in the growth solution. Similar behavior also occurred at pH 11.0 and 11.5 (data not shown). For the pH values studied, the best condition for maximum Ag growth on the surface with minimal Ag nucleation and growth in the solution was found to be at pH 10.6.

Figure 2 shows representative SEM images of Ag nanostructures grown on Si substrates from solutions of different pH as described in Figure 1. The SEM images of structures grown at pH 7.0, 8.0, and 9.1 (frames A−C of Figure 2, respectively) show a few structures that are relatively small, consistent with the low absorbance in Figure 1 and the fact that the ascorbic acid reducing strength is not great enough to reduce Ag^+ appreciably at that pH. The few structures present are mostly small particles. In contrast, the SEM images for structures grown at pH 10.0 (Figure 2D) and pH 10.6 (Figure 2E) show a much greater coverage of larger Ag structures on the surface, including the presence of high aspect ratio (AR) Ag NRs (AR < 20) and NWs (AR ≥ 20). This is consistent with the larger absorbance in the UV−vis at these pH values and a seed-mediated growth mechanism on the surface. The surface at pH 11.9 has a lower coverage compared to that at pH 10.0 and 10.6 but a higher coverage and larger particle size compared to that at pH 7.0, also consistent with the UV−vis data in Figure 1. The coverage of particles on all of the samples should be equal to the initial seed coverage. The differences arise from the fact that the initial seed is too small to observe by SEM. The particles that are observed at lower pH may be due to the small population of seeds that grew to a larger, visible size, leading to the appearance of low coverage. At higher pH, all particle should grow, leading to a surface coverage equal to the initial seed coverage. Although NRs/NWs are present on the surface from pH 10.0 to 11.9, the optimal condition for the highest yield of high-AR 1D structures is ∼pH 10.6.

Figure 3 shows a plot of the average diameter of Ag nanoparticles on the surface and the average coverage of nanostructures on the surface (in number of nanostructures per μm^2) as a function of pH obtained by averaging at least 10 regions of at least three different samples at each pH. (See Table S1 and Figure S2 in Supporting Information for complete data.) The average diameters of the Ag nanoparticles are 20 ± 13, 18 ± 16, 20 ± 16, 27 ± 7, 35 ± 4, and 47 ± 4 for samples A−F, respectively, that are shown in Figure 2. This shows a general increase in growth with increasing pH as expected. The coverage of nanostructures as a function of pH follows the same trend in absorbance observed in Figure 1, where the coverage is very low

(69) Nikhil, R. J.; Gearheart, L.; Murphy, C. J. *Chem. Commun.* **2001**, 617−618.
(70) Lee, G.-J.; Shin, S.-I.; Kim, Y.-C.; Oh, S.-G. *Mater. Chem. Phys.* **2004**, *84*, 197−204.

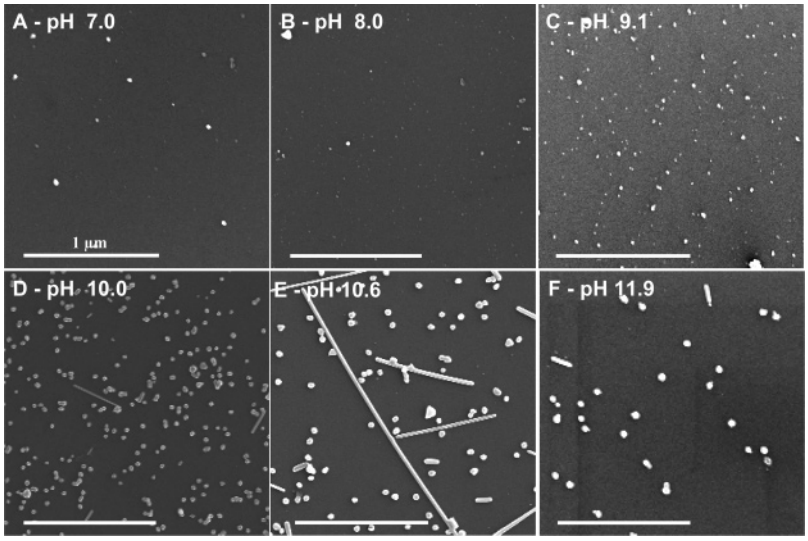

Figure 2. SEM images of Ag nanostructures synthesized at the following pH values: (A) 7.0, (B) 8.0, (C) 9.1, (D) 10.0, (E) 10.6, and (F) 11.9. The scale bar is 1 μm.

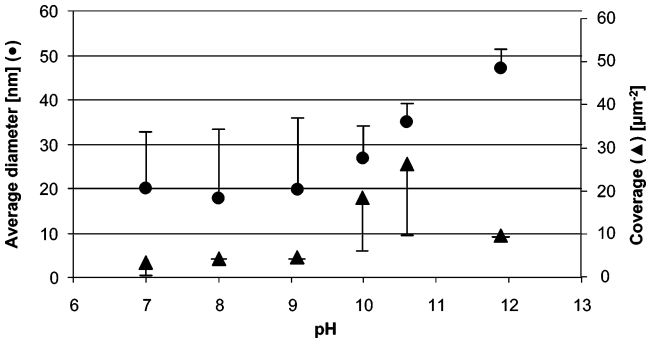

Figure 3. Plots of (●) average diameter and (▲) coverage of Ag nanostructures as a function of the pH of the growth solution.

at pH 7.0, 8.0, and 9.1, highest at pH 10.0 and 10.6 (maximum), and then smaller again at pH 11.9. The low coverage but large diameter of structures at pH 11.9 shows that not many structures grow on the surface but those that do become large. This leads to an overall lower absorbance compared to that at pH 10.0 and 10.6 but a higher absorbance compared to that at pH 7.0.

For samples synthesized at pH 10.6, the Ag NRs/NWs range greatly in length from 50 nm to more than 10 μm with a diameter of approximately 35 nm, giving a range of AR from 1.4 to more than 300. The yield of NR/NWs calculated from five samples is ~3%, which is lower when compared to the 8−15% yield for Au NRs grown similarly.[7,9,16,18,24] Of the 1D structures grown, approximately 40% are NRs (AR < 20), and 60% are NWs (AR ≥ 20). In comparison to our previous results for Au NRs, the coverage for the Ag samples is higher. The average coverage calculated for samples synthesized at pH 10.6 is 26 ± 17 per μm^2, which is approximately 2.5 times as dense compared to our previous results for Au (~10/μm^2).[7] Because the Au seed particles were deposited in an identical manner, this indicates that some Ag structures may form in solution and deposit on the surface or Ag may self-nucleate and grow on the surface during this procedure. Control experiments on slides placed in Ag growth solution without Au NP seeds show almost no growth (Figures S3 and S4 in Supporting Information). We did not obtain high-resolution transmission electron microscopy images of the Ag NRs and NWs to confirm the crystal structure. On the basis of literature results for Au and Ag 1D NRs and NWs similarly synthesized in the presence of surfactants and polymers, we presume that they are not single crystals but instead are multiply twinned structures with 5-fold symmetry where the cross section is a pentagonal shape, the ends of the NRs/NWs contains five (111) facets, and the long axis contains five (100) facets.[23,26,33,34] These 1D structures are thought to grow from multiply twinned decahedral particles along the ⟨110⟩ direction.[25]

Alignment of Silver Nanorods/Nanowires. We previously described the synthesis of highly aligned Au NRs and, more briefly, Ag NRs directly on surfaces using a slight alteration in the surface chemistry from the procedure shown in Scheme 1.[9] First, we functionalized the Si(100) with aminopropyltriethoxy silane (APTES) instead of MPTMS, which renders the surface terminated with NH_2 groups. The surface NH_2 groups were then reacted with acetic acid to form an amide bond with the COOH groups, leaving the surface terminated with CH_3 groups. Exposing the surface to a solution of Au seed nanoparticles leads to the attachment of the seeds to NH_2 groups that did not react during the amidation reaction. Subsequent growth leads to highly aligned NRs on the surface through a mechanism that is not understood at this time.[9] Figure 4 shows an SEM image of a regular (Figure 4A,B) sample of Ag NRs and NWs as compared to an aligned (Figure 4C,D) sample of Ag NRs and NWs that were synthesized directly on Si(100) at pH 10.6 using the revised surface chemistry described. Figure 4A,B clearly shows random orientation, whereas Figure 4C,D shows a preferred growth direction. Ag NRs/NWs (67 ± 5%) are oriented in the same direction within a ±30° range from the alignment direction, which is close to our previously reported value.[9] The yield of NRs/NWs increased slightly from 3 to 5% from regular to aligned samples, and the coverage decreased from 26 ± 17 to 7 ± 2 per μm^2 because many of the surface NH_2 sites became unavailable for seed deposition following the amidation reaction. The average diameter of nanostructures remained similar at 35 nm.

Our procedure is a simple way to assemble and align 1D Ag nanostructures directly on surfaces, but the high population of spherical structures and structures with other shapes on the surface is a major drawback. We previously showed that we could remove many of the spherical particles from 1D structures in the case of Au NRs by applying adhesive tape to the surface and pulling the tape back off.[8] We attempted this with the aligned Ag NRs and NWs and obtained similar results. Figure 4E,F shows SEM images at two different magnifications of samples containing aligned Ag NRs and NWs that had adhesive tape placed on them and removed by pulling back slowly at 180° three times. The

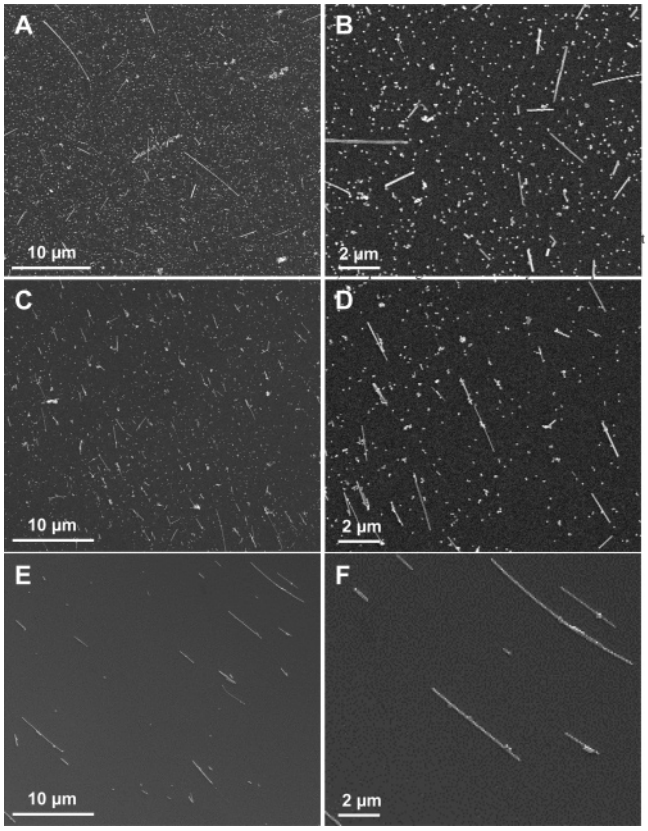

Figure 4. Representative SEM images at two different magnifications of (A, B) regular, (C, D) aligned, and (E, F) aligned and taped (three times) samples of Ag NRs/NWs synthesized on Si/SiO_x surfaces in pH 10.6 buffered growth solution.

images clearly show that this procedure removed a large portion of spherical particles, leaving the surface with 36 ± 13% of NRs and NWs (calculated from 20 random areas) as compared to 5% before taping. Either the spherical particles are attached more weakly to the surface compared to the 1D structures or they form better adhesive contact to the tape.

Formation of Platinum and Palladium 1D Nanostructures by Galvanic Exchange. One of our goals is to extend the synthesis of 1D nanoscale metals directly on surfaces to metals other than Au and Ag and eventually to metal oxides as well. Pt and Pd are attractive metals because they are useful in catalysis,[71] hydrogen storage,[72−74] and hydrogen sensing.[75,76] There have not been any reports to our knowledge on the direct synthesis of Pt and Pd NRs or NWs using seed-mediated growth in solution or directly on surfaces. However, it is possible to convert Ag nanostructures into Pt and Pd by galvanic exchange reactions. Xia and co-workers described the synthesis of 1D nanostructures with well-defined hollow interiors by the galvanic exchange of Ag NWs synthesized by the polyol process with Pd, Pt, and Au salts;[53−59] however, most of these materials were synthesized in solution, and the assembly of these structures was not fully addressed. A simple, quick method for forming surface-assembled Pt and Pd 1D structures is to synthesize Ag 1D structures first directly on surfaces as we described earlier and then convert these structures into Pt and Pd by galvanic exchange. The galvanic exchange reactions are the following:

$$2Ag^0(s) + PtCl_4^{2-}(aq) \leftrightarrow Pt^0(s) + 2AgCl(s \text{ or } aq) + 2Cl^- \quad E^0_{cell} = 0.508\ V^{77} \quad (1)$$

$$2Ag^0(s) + PdCl_4^{2-}(aq) \leftrightarrow Pd^0(s) + 2AgCl(s \text{ or } aq) + 2Cl^- \quad E^0_{cell} = 0.401\ V^{77} \quad (2)$$

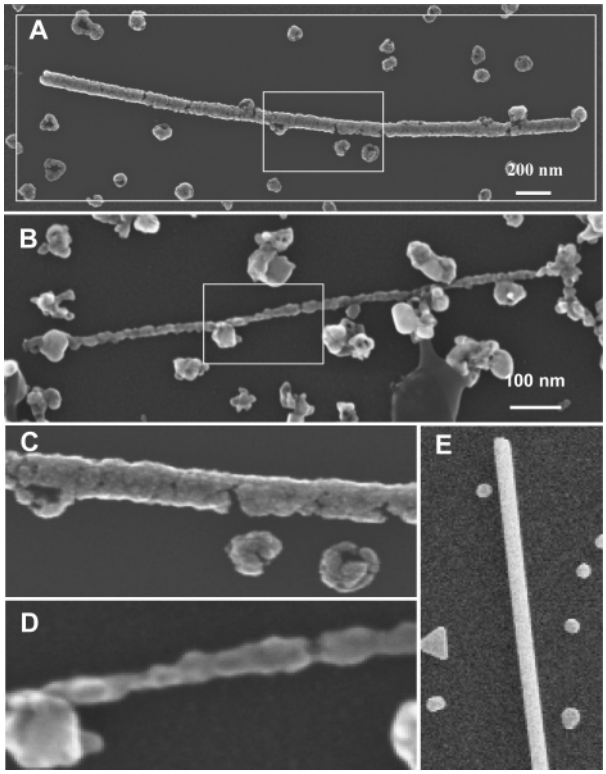

Figure 5. SEM images of Ag NRs/NWs synthesized directly on surfaces after galvanic exchange with (A, C) palladium and (B, D) platinum salts. Frame E shows an original Ag NW with which to compare the morphology.

Part A and B of Figure 5 show SEM images of Ag NRs/NWs exchanged with Pd and Pt, respectively. The exchange occurred by simply placing as-prepared Ag NR/NW samples into a 0.005 M solution of $PdCl_4^{2-}$ and $PtCl_4^{2-}$ for 5 min to form Pd and Pt nanostructures, respectively. Frames C and D of Figure 5 show expanded images of the Pd and Pt NR/NWs. The smooth, semicrystalline, and uniform-diameter Ag 1D nanostructures (Figures 2 and 5E) become rough, porous, and polycrystalline Pd- and Pt-containing structures following galvanic exchange. After exchange with Pd or Pt, there are noticeable cracks, pits, and other defects in the rods, wires, and neighboring particles. The Pd structures especially appear to be hollow as previously observed for solution-phase Ag NWs exchanged galvanically with Pd, although this needs to be confirmed with TEM.[54] The nanostructures importantly retained their general 1D shape after galvanic exchange directly on surfaces. This morphology should be beneficial for sensing and catalysis applications because of the higher surface area and potentially more active surface in comparison to smooth, crystalline structures.

Frames A and B of Figure 6 show UV−vis data of Ag NR/NW samples grown on glass before and after exchange with platinum and palladium salts, respectively, as a function of time. The plot labeled "Ag" is before exchange, where the surface

(71) Liu, Z.; Hong, L.; Tham, M. P.; Lim, T. H.; Jiang, H. *J. Power Sources* **2006**, *161*, 831−835.
(72) Dresselhaus, M. S.; Thomas, I. L. *Nature* **2001**, *414*, 332−337.
(73) Schlapbach, L.; Zuttel, A. *Nature*, **2001**, *414*, 353−358.
(74) Ward, M. D. *Science* **2003**, *300*, 1104−1105.
(75) Weiss, A.; Ramaprabhu, S.; Rajalakshmi, N. Z. *Phys. Chem.* **1997**, *199*, 165.
(76) Lauhon, L. J.; Gudiksen, M. S.; Wang, D.; Lieber, C. M. *Nature* **2002**, *420*, 57−61.

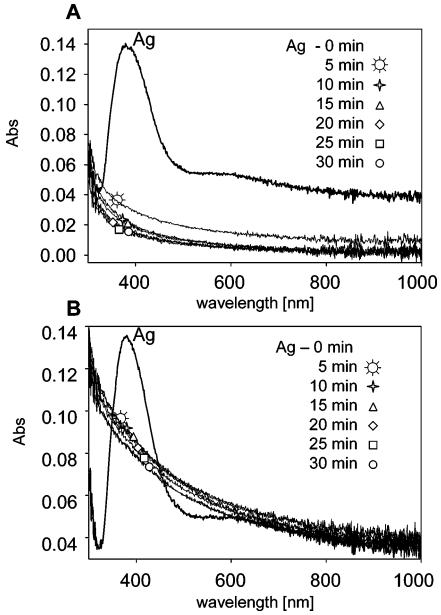

Figure 6. UV−vis spectra of Ag NR/NW samples before and after exchange with (A) platinum and (B) palladium salts at 0.005 M concentration as a function of time.

plasmon (SP) band at ∼400 nm is clearly observed for the Ag nanostructures. After 5 min of exchange with Pt or Pd, the Ag SP band completely disappears, and the spectrum shows a featureless exponential decrease in absorbance as the wavelength increases, as expected for pure (or those containing a high content of) Pt or Pd nanostructures. This indicates that Ag is mostly exchanged after 5 min. Small additional changes occur over the next 25 min, however, indicating that the structures may still be PdAg or PtAg alloys. X-ray photoelectron spectroscopy (XPS) data confirmed the existence of Pt and Pd on the surface after 5 min of exchange, but also showed the presence of some Ag as well (data not shown). This could be due to the reaction not going to completion or the presence of solid AgCl left on the surface, which has low solubility in water. Xia and co-workers showed that performing the galvanic exchange of Ag NWs with Au salt at higher temperatures leads to the removal of AgCl solid, leaving gold nanoshells free of contamination from AgCl.[55] They observed rough features containing leftover AgCl at room temperature, consistent with our results. We are currently studying the exchange process as a function of temperature and Pd and Pt salt concentration to understand the kinetics of the process and determine how these factors affect the final morphology of the exchanged structure. We will report these findings in a future publication. For this article, we wanted to demonstrate the synthesis of other metal 1D nanostructures, such as Pd and Pt, by galvanic exchange. Ag can also be exchanged with Au to synthesize more-porous 1D Au structures on surfaces (data not shown).

Formation of Au/Pd Core/Shell Nanostructures. Au nanorods, instead of Au nanoparticles, can also serve as seeds for Ag growth. This has led to interestingly shaped Au/Ag core/shell structures reported in the literature.[78] Here we show the synthesis of Au/Pd core/shell NRs directly on surfaces by depositing a Ag shell on Au NRs and then replacing the Ag shell with Pd by galvanic exchange (Scheme 2). Au NRs were first grown directly on the surface by seed-mediated growth as described in our previous work.[7,8,18] Ag was then deposited on

Scheme 2. Procedure for Synthesizing Au/Pd Core/Shell Nanorods

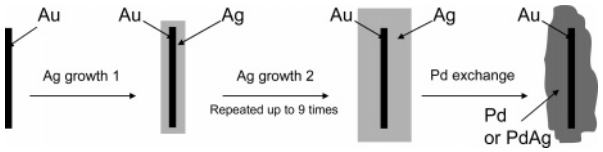

the Au NRs using the procedure described in this article at pH 10.6 for 30 min. This step was performed up to nine times to produces thicker Ag shells. Finally, the Ag was exchanged with Pd by immersion in an aqueous solution of 0.005 M $PdCl_4^{2-}$ for 5 min.

Figure 7 shows the UV−vis spectra of various Au NR samples before and after deposition of Ag by seed-mediated growth and after exchange with palladium. Frame A shows the UV−vis spectrum of an Au NR sample (•••), the same sample after one treatment of Ag seed-mediated growth (−), and the same sample after Pd galvanic exchange for 5 min (---). The spectrum of the Au NR displays an SP band at about 520 nm, as expected for Au nanoparticles and NRs on the surface. Following the seed-mediated growth of Ag, the SP band at 520 nm shifts to 500 nm, and a new peak appears at about 350 nm. This is consistent with what has been observed and is predicted for Au/Ag core/shell structures.[79] The peak at 350 nm has been commonly observed for 1D Ag nanostructures.[27,30,31,80] After Pd exchange, the peak at 350 nm disappears, and a new peak appears at about 560 nm. The loss of the Ag peak at 350 nm is consistent with removal of Ag by galvanic exchange with Pd. We attribute the new peak at 560 nm to the Au SP band that has been altered by the porous Pd shell surrounding the Au. Previously, Yang and co-workers deposited Pd directly on Au NRs by seed-mediated growth but observed a featureless UV−vis spectrum because Pd does not normally exhibit a prominent SP band in the visible range.[81] Our results may be different because of the different morphology and manner in which Pd coats the Au NRs in our case. Previous exchange of (AuAg alloy)/Ag (core)/shell nanoparticles with Pd led to nanorattles, where the AuAg core is disconnected from the hollow PdAg shell.[59] Our structures may be similar, which is drastically different from direct deposition of Pd on Au and could alter the optical properties.

Frames B−D of Figure 7 show UV−vis spectra of Au NR samples before and after treatment with Ag growth solution three, five, and nine times, respectively, and then after exchange with Pd. All of the Au NR samples (•••) again show a transverse plasmon band at 520 nm. After depositing Ag (−), the Au SP band shifts to lower wavelengths and the new Ag SP band appears at around 350 nm. The Au SP band shifts to lower wavelengths and the Ag SP band shifts to higher wavelengths with an increasing number of exposures to Ag growth solution. The Ag SP eventually dominates the spectra with increasing amounts of Ag, but the Au SP band remains visible even after nine exposures to Ag growth solution. We exchanged each Au NR sample containing varying amounts of Ag with Pd. As in frame A, the Ag SP band disappears, and a peak appears ranging from 560 to 640 nm, depending on the amount of Ag deposited. We attribute this peak to the Au in the core of the Au/Pd core/shell nanostructure, which shifts to longer wavelengths with an increasing amount of Pd in the

(77) *CRC Handbook of Chemistry and Physics*, 63rd ed.; CRC Press: Boca Raton, FL, 1982−1983; pp D162−D167.
(78) Huang, C.-C.; Yang, Z.; Chang, H.-T. *Langmuir* **2004**, *20*, 6089−6092.
(79) Bright, R. M.; Walter, D. G.; Musick, M. D.; Jackson, M. A.; Allison, K. J.; Natan, M. J. *Langmuir* **1996**, *12*, 810−817.
(80) Gao, Y.; Jiang, P.; Liu, D. F.; Yuan, H. J.; Yan, X. Q.; Zhou, Z. P.; Wang, J. X.; Song, L.; Liu, L. F.; Zhou, W. Y.; Wang, G.; Wang, C. Y.; Xie, S. S.; Zhang, J. M.; Shen, D. Y. *J. Phys. Chem. B* **2004**, *108*, 12877−12881.
(81) Song, J. H.; Kim, F.; Kim, D.; Yang, P. *Chem.—Eur. J.* **2005**, *11*, 910−916.

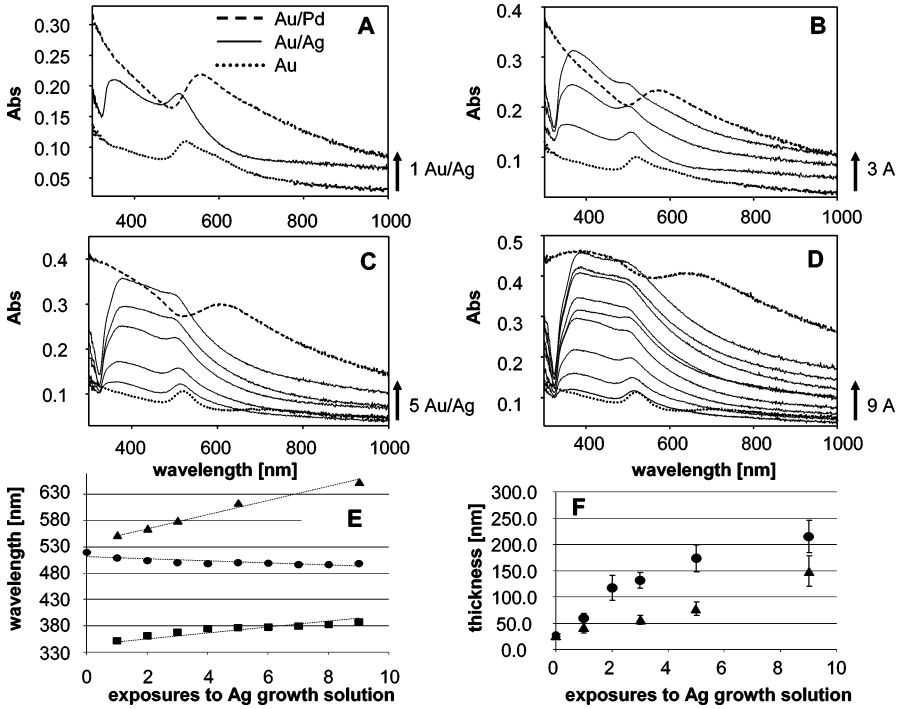

Figure 7. UV−vis spectra of Au NR samples before and after Ag deposition and after palladium exchange. The Au NRs were exposed to the pH 10.6 Ag growth solution one, three, five, and nine times for frames A−D, respectively. Frame E shows the shift in wavelength for the (●) gold peak, (■) developing silver peak, and (▲) peak after palladium exchange as a function of the number of exposures to Ag growth solution. Frame F shows the thickness of the NRs/NWs (▲) after Ag deposition and (●) after Pd exchange as a function of the number of exposures to Ag growth solution.

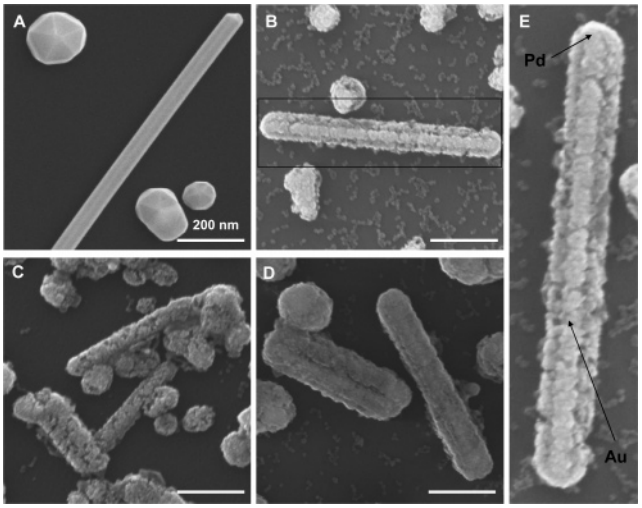

Figure 8. SEM images of Si/SiO_x samples containing Au NRs before (A) and after exposure to pH 10.6 Ag growth solution for 30 min once (B), twice (C), and three times (D), followed by exposure to a 0.005 M $PdCl_4^{2-}$ solution for 5 min. The scale bar is 200 nm for all graphs. (E) The SEM image is a magnification of frame B to show the core/shell structure of the Au/Pd NRs better.

shell. Figure 7E shows a plot of the Au and Ag SP band of the Au/Ag core/shell structures before and after Pd exchange as a function of the number of exposures to Ag growth solution. This shows the general trend of the Au SP band decreasing in wavelength with increasing Ag (●), the Ag SP band increasing in wavelength with increasing Ag (■), and the Au SP band after Pd exchange increasing in wavelength with increasing amounts of Ag (or Pd) (▲). Figure 7F shows the thickness of the Au/Ag core/shell NRs and the thickness of the corresponding Au/Pd core/shell NRs after exchange as a function of exposure to Ag growth solution. The Au NRs are originally about 30 nm in diameter (no exposure). The diameter increases fairly linearly to a maximum diameter of about 150 nm after nine cycles in Ag growth solution (▲), and the corresponding Au/Pd core/shell NRs increase to a maximum value of 210 nm (●) after nine cycles in Ag growth followed by Pd exchange.

Figure 8 shows SEM images of the Au NRs (frame A) and the Au/Pd core/shell NRs after 1−3 exposures to Ag growth solution followed by Pd exchange (frames B−D, respectively). The original Au NRs have smooth morphology with a highly uniform diameter along the length of the NR. In contrast, the Au/Pd NRs have rough morphology that noticeably increases in thickness with increasing exposure to Ag before Pd exchange. Figure 8E shows an expanded image of an Au/Pd core/shell NR (one exposure to Ag) where there is significant contrast between the Au core and Pd shell to distinguish between them.

Conclusions

In this report, we described the effect of pH on the seed-mediated growth of Ag NRs/NWs synthesized directly on surfaces. Ag NRs/NWs grow optimally at pH 10.6 under our conditions as confirmed by UV−vis spectroscopy and SEM. The yield is very low (3%), and there is considerable dispersity in length, ranging from as short as 50 nm to as long as 10 μm, whereas the diameter is fairly uniform at about 35 nm. The large dispersity in length and low yield of rods/wires remain problems, but the method is useful for assembling well-separated 1D nanostructures directly on surfaces and we improved the percentage of 1D structures on the surface to 36% by using adhesive tape to remove other shapes. Altering the surface chemistry leads to the growth of highly aligned Ag NRs (~67% in the same direction) directly on surfaces. The Ag NRs/NWs also served as templates for the formation of high-surface-area Pd and Pt 1D nanostructures through galvanic exchange reactions. In addition, we described an approach to synthesizing interesting Au/Pd core/shell NRs directly on surfaces by combining the Ag

seed-mediated growth on Au NRs followed by galvanic exchange with Pd. Surface-attached metal nanostructures have a wide range of potential uses. Extending our method of synthesizing metal 1D nanostructrures directly on surfaces to Ag, Pt, Pd, and Au/Pd core/shell structures could open up applications for these materials in catalysis, hydrogen sensing, hydrogen storage, nanoelectronics, chemical sensing, and surface-enhanced Raman spectroscopy (SERS).

Acknowledgment. We gratefully acknowledge the National Science Foundation (CHE-0518561) and the donors of the American Chemical Society Petroleum Research Fund for support of this research. We thank Dr. Mahendra K. Sunkara from the Department of Chemical Engineering at the University of Louisville for the use of the X-ray photoelectron spectrometer (XPS) and Suresh Gubbala for assistance in acquiring the XPS data. We also acknowledge Dr. Robert Cohn from the Department of Electrical and Computer Engineering at the University of Louisville for granting us access to the Scanning Electron Microscope, and we thank Dr. Aneta J. Mieszawska for assistance with the alignment procedure.

Supporting Information Available: Expanded view of low-absorbance spectra from Figure 1B, measured Ag nanostructure coverage for all samples synthesized at various pH values, SEM images showing examples of different coverages observed in different regions of a sample synthesized at pH 10.0, and SEM images comparing the growth of Ag NRs/NWs on surfaces with and without Au seeds. This material is available free of charge via the Internet at http://pubs.acs.org.

LA701606P